

ORDER, DISORDER, AND PHASE TRANSITION  
IN CONDENSED SYSTEM

Magnetic Anisotropy and Magnetoelectric Properties  
of  $Tb_{1-x}Er_xFe_3(BO_3)_4$  Ferroborates

A. K. Zvezdin<sup>b</sup>, A. M. Kadomtseva<sup>a</sup>, Yu. F. Popov<sup>a</sup>, G. P. Vorob'ev<sup>a</sup>, A. P. Pyatakov<sup>a,b</sup>,  
V. Yu. Ivanov<sup>b</sup>, A. M. Kuz'menko<sup>b</sup>, A. A. Mukhin<sup>b</sup>, L. N. Bezmaternykh<sup>c</sup>, and I. A. Gudim<sup>c</sup>

<sup>a</sup> Moscow State University, Moscow, 119992 Russia

<sup>b</sup> Prokhorov Institute of General Physics, Russian Academy of Sciences, Moscow, 119991 Russia

<sup>c</sup> Kirenskii Institute of Physics, Siberian Division, Russian Academy of Sciences, Krasnoyarsk, 660038 Russia  
e-mail: kadomts@plms.phys.msu.ru

Received November 24, 2008

**Abstract**—Magnetic and magnetoelectric properties of ferroborate single crystals with complex composition ( $Tb_{1-x}Er_xFe_3(BO_3)_4$ ,  $x = 0, 0.75$ ) and with competing exchange Tb–Fe and Er–Fe interactions are investigated. Jumps in electric polarization, magnetostriction, and magnetization are observed as a result of spin-flop transitions, as well as a considerable decrease in the critical field upon an increase in the Er concentration, in a field  $H_c$  parallel to the  $c$  axis. The observed behavior of phase-transition fields is analyzed and explained using a simple model taking into account anisotropy in  $g$  factors and exchange splitting of fundamental doublets of the easy-axis  $Tb^{3+}$  ion and easy-plane  $Er^{3+}$  ion. It is established that magnetoelectric and magnetostriction anomalies under spin-flop transitions are mainly controlled by the Tb subsystem. The Tb subsystem makes a nonmonotonic contribution  $\Delta P_a(H_a, T)$  to polarization along the  $a$  axis: the value of  $\Delta P_a$  reverses its sign and increases with temperature due to the contribution from the excited states of the  $Tb^{3+}$  ion.

PACS numbers: 75.80.+q

DOI: 10.1134/S1063776109070097

1. The magnetic, magnetoelectric, and many other properties of new multiferroics  $RFe_3(BO_3)_4$  with a rhombohedral structure described by trigonal space groups  $R32(D_3^7)$  or  $P3_121(D_3^4)$  have been intensely studied in recent years [1–6]. The spins of  $Fe^{3+}$  ion below the Néel temperature  $T_N \approx 30\text{--}40$  K in ferroborates are ordered antiferromagnetically; the orientation of these ions is considerably affected by anisotropic properties of the paramagnetic subsystem of the rare-earth R ion, which may stabilize either easy-plane states in the  $ab$  plane of the crystal (e.g., for R = Nd [2, 7–10] and Er [11]) or uniaxial states with spins parallel to the trigonal  $c$  axis (R = Tb [12, 13], Dy [14], and Pr [6]) owing to the R–Fe exchange interaction.

In this connection, it would be interesting to study the change in magnetic anisotropy and magnetoelectric properties of complex ferroborates with two competing types of rare-earth ions stabilizing different magnetic structures. By way of example, we consider  $Tb_{0.25}Er_{0.75}Fe_3(BO_3)_4$ . The concentration of  $Fe^{3+}$  ions (75%) is chosen from the condition of approximate equality of contributions from two rare-earth subsystems to anisotropy.

2. Single crystals of  $Tb_{1-x}Er_xFe_3(BO_3)_4$  ferroborates ( $x = 0, 0.75$ ) were obtained as a result of spontaneous crystallization from solutions in melts [15]. Magnetic, magnetoelectric, and magnetoelastic prop-

erties were analyzed in pulsed magnetic fields of up to 250 kOe as well as in static fields of up to 50 kOe on a MPMS-5 SQUID magnetometer (Quantum Design); a vibration magnetometer was used for static fields of up to 14 kOe. For measuring magnetostriction  $\lambda$  and electric polarization  $\Delta P$  in a pulsed magnetic field, epoxy resin electrodes with a conducting filler were deposited on the faces of the sample under investigation, which were perpendicular to the direction in which  $\Delta P$  was measured. Magnetostriction was measured by a piezoelectric sensor in the form of a monocrystalline quartz plate glued to the same faces, which perceived deformation only in one direction (in which magnetostriction  $\lambda(H)$  was measured). The charge induced on the sample as a result of the magnetoelectric effect or on the quartz piezoelectric sensor due to magnetostrictive deformation of the sample was fed via an electrometer to an analog-to-digital converter. The time of leakage of the charge from the sample for magnetic field pulse durations of  $t_p \sim 10^{-2}$  s used in our experiments was two or three orders of magnitude longer than the measurement time, which ensured reliability of results. The measuring technique in pulsed fields is described in greater detail in [16]. Comparison of the magnetic field dependences of magnetization  $M(H)$  and polarization  $\Delta P(H)$  measured by static methods with the help of the SQUID magnetometer and in a pulsed magnetic field revealed complete matching (except for the width of the hysteresis).

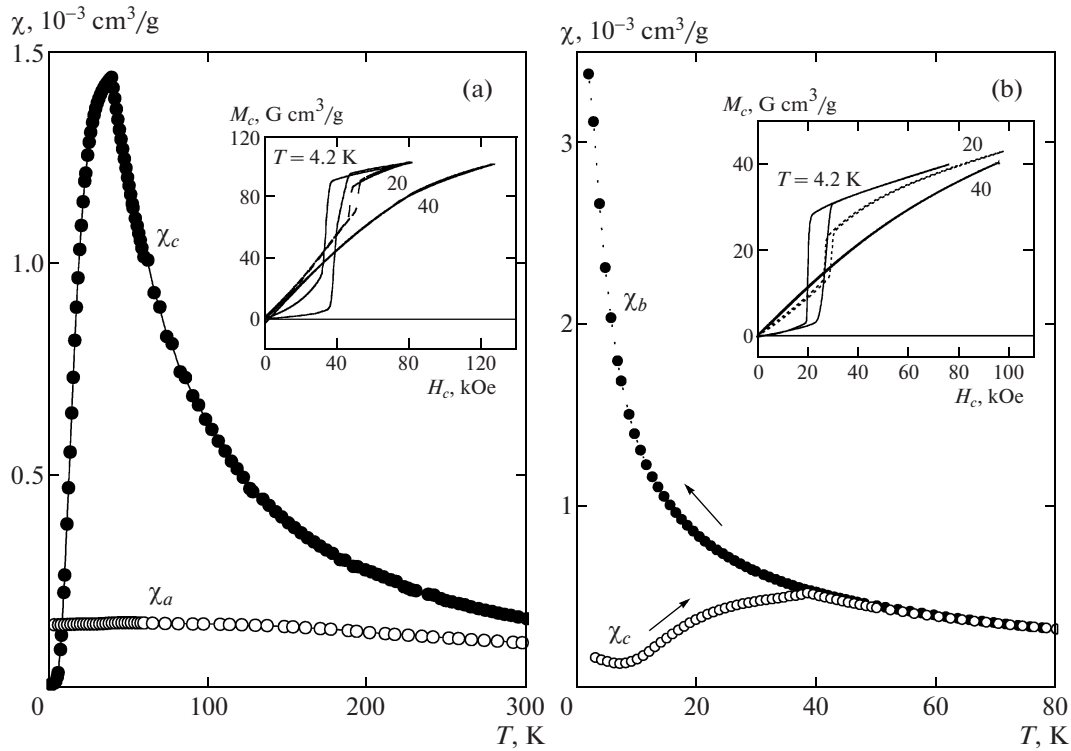


**Fig. 1.** Temperature dependences of magnetic susceptibility ( $\chi_c$ ) and ( $\chi_a$ ) along the  $c$  axis and at right angles to it in (a)  $\text{TbFe}_3(\text{BO}_3)_4$  and (b)  $\text{Tb}_{0.25}\text{Er}_{0.75}\text{Fe}_3(\text{BO}_3)_4$ , measured in a field of 1 kOe. The insets show examples of magnetization curves along the  $c$  axis illustrating spin-flop transitions.

esis loop) of the curves to within the experimental error, indicating that the magnetocaloric effect is weak and relaxation (nonstationary) processes in pulsed fields are insignificant for the compositions studied here.

**3.** Figure 1 shows the temperature dependences of the magnetic susceptibility ( $\chi_c$ ) and ( $\chi_a$ ) of the compounds along the  $c$  axis and at right angles to it, as well as the curves (in the inset) describing the magnetization along the  $c$  axis. In terbium ferrobortate, in which the  $\text{Tb}^{3+}$  ion is a strongly anisotropic Ising ion (the corresponding  $g$  factors are  $\text{Tb}^{3+}$ ,  $g_x = g_y \approx 0$ ,  $g_z = 17.5$ – $17.8$  [12]), the spins of  $\text{Fe}^{3+}$  ions at  $T < T_N = 40$  K are oriented under the effect of the Tb–Fe exchange in the same way as the  $\text{Tb}^{3+}$  ion (i.e., along the trigonal  $c$  axis). Measurement of the temperature dependence of the magnetic susceptibility in a constant magnetic field applied along the  $c$  axis of the crystal revealed that  $\chi_c(T)$  increases hyperbolically upon cooling from 300 K to  $T_N$ . For  $T < T_N$ , it sharply decreases and vanishes almost entirely at 2 K (Fig. 1a). Susceptibility  $\chi_a$  is much smaller than  $\chi_c$  at all temperatures except the lowest ones and varies smoothly with temperature. The observed behavior of the susceptibility fully confirms the Ising type of  $\text{Tb}^{3+}$  ion at low temperatures and is in conformity with the results obtained in [12, 13]. The noticeable decrease observed in  $\chi_c(T)$  at

$T < T_N$  is obviously associated with exchange splitting of the fundamental quasi-doublet of the  $\text{Tb}^{3+}$  ion upon antiferromagnetic spin ordering of  $\text{Fe}^{3+}$  ions, resulting in antiparallel (antiferromagnetic) polarization of  $\text{Tb}^{3+}$  ions in the corresponding sublattices.

The magnetization curves  $M_c(H_c)$  of terbium ferrobortate along the  $c$  axis (see the inset to Fig. 1a) display sharp magnetization jumps corresponding to spin flop of the  $\text{Fe}^{3+}$  ions to the basal plane, which is accompanied by reversal of magnetization of the magnetic moments of the  $\text{Tb}^{3+}$  ions [12, 13]. The transition field is about 35 kOe at 2 K and increases with temperature.

Let us now consider the properties of single crystals with the substituted composition  $\text{Tb}_{0.25}\text{Er}_{0.75}\text{Fe}_3(\text{BO}_3)_4$ . It can be seen from Fig. 1b that the magnetic susceptibility curve along the  $c$  axis near  $T_N \approx 40$  K has a small kink, after which the magnetic susceptibility strongly decreases at  $T < T_N$ , which is typical of uniaxial praseodymium, terbium, and dysprosium ferrobortates [6, 12–14]. Consequently, the contribution of terbium to uniaxial anisotropy of  $\text{Tb}_{0.25}\text{Er}_{0.75}\text{Fe}_3(\text{BO}_3)_4$  prevails over the contribution of erbium to easy-plane anisotropy, and the compound remains uniaxial in the entire temperature range below  $T_N$ . The conclusion on the uniaxial nature of the substituted crystal is confirmed by the  $M_c(H_c)$  magnetization curves measured in mag-

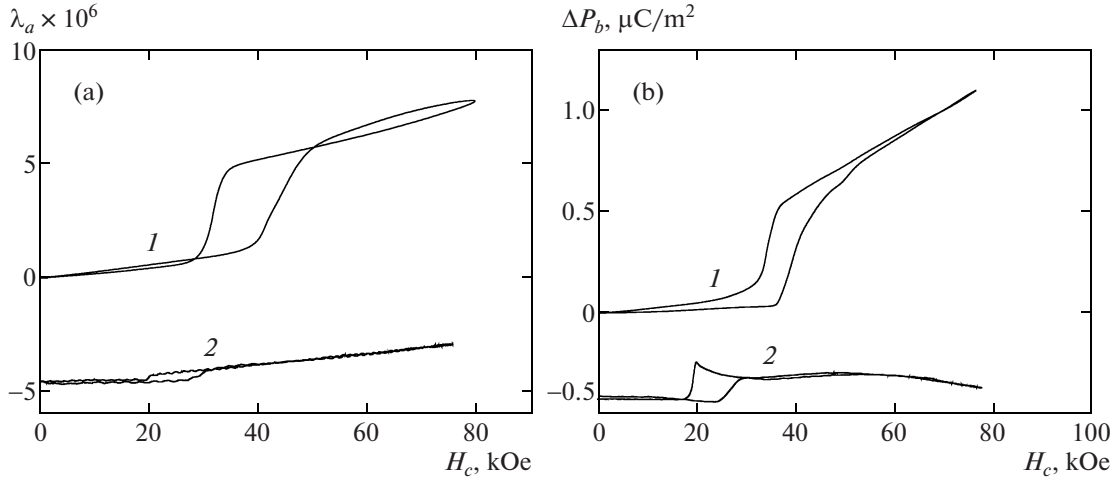


**Fig. 2.** Dependences of (a) magnetostriction along the  $a$  axis and (b) electric polarization along the  $b$  axis on magnetic field directed along the  $c$  axis at  $T = 4.2$  K in  $\text{TbFe}_3(\text{BO}_3)_4$  (curves 1) and  $\text{Tb}_{0.25}\text{Er}_{0.75}\text{Fe}_3(\text{BO}_3)_4$  (curves 2).

netic field  $H_c$ , which exhibit jumpwise variation during a spin-flop transition (see the inset to Fig. 1b). As compared to  $\text{TbFe}_3(\text{BO}_3)_4$ , the magnetization in fields stronger than the spin-flop transition field decreases to almost one-fourth in proportion to the concentration of the  $\text{Tb}^{3+}$  ions (25%), which indicates a very small contribution of the erbium subsystem to  $M_c$ .

Magnetostriction (Fig. 2a) and electric polarization anomalies (Fig. 2b) are also observed during spin-flop transition in both ferroborates; the values of corresponding threshold fields  $H_{sf}$  correlate with the results of magnetic measurements. The  $H_{sf}(T)$  dependences obtained from measurement of the magnetic and magnetoelectric properties and magnetostriction for both compounds are shown in Fig. 3. Comparison of the  $H_{sf}(T)$  phase diagrams for the two compounds shows that the threshold fields for the erbium-substituted terbium ferroborate are much lower than for pure  $\text{TbFe}_3(\text{BO}_3)_4$  due to the contribution from easy-plane  $\text{Er}^{3+}$  ions to anisotropy. The slope of the  $H_{sf}(T)$  curves for the substituted compound is smaller than for  $\text{TbFe}_3(\text{BO}_3)_4$ , which points to a tendency toward transition to the easy-plane state; however, spontaneous reorientation of spins from the  $c$  axis to the basal plane does not take place for the given erbium concentration ( $x = 0.75$ ).

**4.** To describe the observed magnetic properties of  $\text{Tb}_{1-x}\text{Er}_x\text{Fe}_3(\text{BO}_3)_4$  ferroborates, we must take into account the contribution to the thermodynamic potential from not only the antiferromagnetic Fe subsystem, but also from paramagnetic rare-earth ions of both types in external magnetic field  $\mathbf{H}$ , in the exchange field of iron ion spins, and in the crystal field. Since the interaction between rare-earth ions can be disregarded down to the lowest temperatures (of about 1 K), these ions will make an additive contri-

bution to the total thermodynamic potential of the system, which can be represented in the form

$$\Phi(\mathbf{l}, \mathbf{H}) = -\frac{1}{2}\chi_{\perp}^{\text{Fe}}\mathbf{H}^2 + (\chi_{\perp}^{\text{Fe}} - \chi_{\parallel}^{\text{Fe}})(\mathbf{H} \cdot \mathbf{l})^2 + \frac{1}{2}K_{\text{Fe}}l_z^2 - \frac{1}{2}(1-x)Nk_{\text{B}}T \sum_{\alpha=\pm} \ln \left[ 2 \cosh \left( \frac{\Delta_{\text{Tb}}^{\alpha}}{k_{\text{B}}T} \right) \right] - \frac{1}{2}xNk_{\text{B}}T \sum_{\alpha=\pm} \ln \left[ 2 \cosh \left( \frac{\Delta_{\text{Er}}^{\alpha}}{k_{\text{B}}T} \right) \right], \quad (1)$$

where the first three terms define the contribution from the antiferromagnetically ordered Fe subsystem, while the last two terms describe the contribution of rare-earth  $\text{Tb}^{3+}$  and  $\text{Er}^{3+}$  ions considered in the one-doublet approximation;  $\mathbf{l} = (l_{\perp}, l_z)$  is the dimensionless antiferromagnetism vector of iron ions;  $\chi_{\perp}^{\text{Fe}}$ ,  $\chi_{\parallel}^{\text{Fe}}$ , and  $K_{\text{Fe}} > 0$  are the transverse and longitudinal susceptibilities and uniaxial anisotropy constant of the Fe subsystem, respectively;  $2\Delta_{\text{Tb}}^{\pm}$  and  $2\Delta_{\text{Er}}^{\pm}$  are the splittings of the fundamental doublet of the  $\text{Tb}^{3+}$  and  $\text{Er}^{3+}$  ions,

$$\Delta_{\text{Tb}}^{\pm} = \mu_{\text{Tb}}^z H_z \pm \Delta_{\text{Tb}}^z l_z, \quad (2)$$

$$\Delta_{\text{Er}}^{\pm} = \sqrt{(\mu_{\text{Er}}^z H_z \pm \Delta_{\text{Er}}^z l_z)^2 + (\mu_{\text{Er}}^{\perp} H_{\perp} \pm \Delta_{\text{Er}}^{\perp} l_{\perp})^2},$$

$\mu_{\text{Tb, Er}}^z$  and  $\mu_{\text{Er}}^{\perp}$  are the magnetic moments of ions along the  $z$  ( $c$ ) axis and at right angles to it;  $2\Delta_{\text{Tb, Er}}^z$  and  $2\Delta_{\text{Er}}^{\perp}$  are the exchange splittings of the fundamental doublet of the R ions in the uniaxial and easy-plane states of the spins of the Fe subsystem, respectively; signs  $\pm$  correspond to two R sublattices; and  $N$  is the total number of R ions.

Let us first analyze the behavior of pure  $\text{TbFe}_3(\text{BO}_3)_4$  ( $x = 0$ ) in a magnetic field  $H_c$ . For  $T \rightarrow 0$  ( $\chi_{\parallel}^{\text{Fe}} \rightarrow 0$ ), the thermodynamic potential of the system has the form

$$\Phi(\mathbf{l}, \mathbf{H}) = -\frac{1}{2}\chi_{\perp}^{\text{Fe}}[\mathbf{H}^2 - (\mathbf{H} \cdot \mathbf{l}^2)] + \frac{1}{2}K_{\text{Fe}}I_z^2 - \frac{1}{2}N(|\mu_{\text{Tb}}^z H_z + \Delta_{\text{Tb}}^z I_z| + |\mu_{\text{Tb}}^z H_z - \Delta_{\text{Tb}}^z I_z|). \quad (3)$$

From the equality of the potential of the system in the uniaxial ( $I_z = 1$ ) and easy-plane ( $I_{\perp} = 1$ ) states, we obtain the following expression for spin-flop transition field  $H_{\text{sf}}$ :

$$H_{\text{sf}} = \sqrt{\left(\frac{N\mu_{\text{Tb}}^z}{\chi_{\perp}^{\text{Fe}}}\right)^2 + \frac{2N\Delta_{\text{Tb}}^z - K_{\text{Fe}}}{\chi_{\perp}^{\text{Fe}}} - \frac{N\mu_{\text{Tb}}^z}{\chi_{\perp}^{\text{Fe}}}} \approx \frac{\Delta_{\text{Tb}}^z}{\mu_{\text{Tb}}^z} \left(1 - \frac{K_{\text{Fe}}}{2N\Delta_{\text{Tb}}^z}\right). \quad (4)$$

Here, we took into account the fact that  $\chi_{\perp}^{\text{Fe}} H_{\text{sf}}^2 \ll 2N\Delta_{\text{Tb}}^z$  ( $\chi_{\perp}^{\text{Fe}} \approx 1.25 \times 10^{-4} \text{ cm}^3/\text{g}$  in  $\text{YFe}_3(\text{BO}_3)_4$  [15] and  $2\Delta_{\text{Tb}}^z \approx 30 \text{ cm}^{-1}$  [12]). In addition, assuming that the anisotropy constant is small,  $K_{\text{Fe}} \approx 2.9 \times 10^5 \text{ erg/g}$  ( $1.2 \text{ cm}^{-1}/\text{formula unit}$ ) [6, 17], as compared to the exchange splitting of the fundamental doublet of the  $\text{Tb}^{3+}$  ion, we can conclude that the spin-flop transition field at low temperatures is close to the exchange splitting field,  $H_{\text{sf}} \approx \Delta_{\text{Tb}}^z / \mu_{\text{Tb}}^z \approx 35 \text{ kOe}$ , where  $\mu_{\text{Tb}}^z \approx (8.6\text{--}8.8)\mu_{\text{B}}$ ; i.e., spin flop in iron ions occurs in the vicinity of the magnetization-reversal field of the Tb sublattice with the magnetization antiparallel to the external field.

At high temperatures ( $\Delta_{\text{Tb}}^{\pm} \ll k_{\text{B}}T$ , the expression for thermodynamic potential is simplified as follows:

$$\Phi(\mathbf{l}, \mathbf{H}) = -\frac{1}{2}\chi_{\perp}^{\text{Fe}}\mathbf{H}^2 + (\chi_{\perp}^{\text{Fe}} - \chi_{\parallel}^{\text{Fe}})(\mathbf{H} \cdot \mathbf{l})^2 + \frac{1}{2}K_{\text{eff}}I_z^2 + \dots, \quad (5)$$

and the spin-flop transition field is defined by the classical expression

$$H_{\text{sf}} = \sqrt{\frac{K_{\text{eff}}}{\chi_{\perp}^{\text{Fe}} - \chi_{\parallel}^{\text{Fe}}}}, \quad (6)$$

where  $K_{\text{eff}} = K_{\text{Fe}} - N(\Delta_{\text{Tb}}^z)^2/k_{\text{B}}T < 0$  is the effective anisotropy constant stabilizing the uniaxial phase due to exchange splitting of the doublet of the  $\text{Tb}^{3+}$  ion. The observed increase in the threshold field upon heating (see Fig. 3) stems from a decrease in the difference in susceptibilities  $\chi_{\perp}^{\text{Fe}} - \chi_{\parallel}^{\text{Fe}}$ .

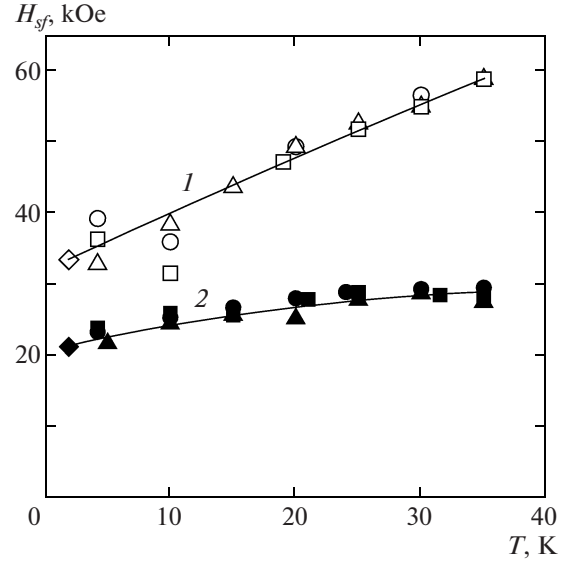


Fig. 3. Temperature dependences of the threshold field of the spin-flop transition in  $\text{TbFe}_3(\text{BO}_3)_4$  (1) and  $\text{Tb}_{0.25}\text{Er}_{0.75}\text{Fe}_3(\text{BO}_3)_4$  (2) obtained from measured magnetization ( $\circ$ ,  $\bullet$ —pulsed fields;  $\diamond$ ,  $\blacklozenge$ —SQUID magnetometer), magnetostriction ( $\triangle$ ,  $\blacktriangle$ ), and electric polarization ( $\square$ ,  $\blacksquare$ ).

Let us now consider the substituted system  $\text{Tb}_{1-x}\text{Er}_x\text{Fe}_3(\text{BO}_3)_4$ . In the high-temperature approximation, the spin-flop transition field is also defined by expression (6) with a renormalized anisotropy constant:

$$K_{\text{eff}} = K_{\text{Fe}} - \frac{N}{k_{\text{B}}T}[(1-x)(\Delta_{\text{Tb}}^z)^2 - x(\Delta_{\text{Er}}^{\perp})^2 - (\Delta_{\text{Er}}^z)^2].$$

The absolute values of  $K_{\text{eff}}$  and of threshold field  $H_{\text{sf}}$  decrease due to anisotropy in exchange splitting of the fundamental doublet of the  $\text{Er}^{3+}$  ion; according to the spectroscopic data for the  $\text{ErFe}_3(\text{BO}_3)_4$  and other ferroborates with an erbium impurity [11], this splitting is  $2\Delta_{\text{Er}}^{\perp} \approx 6.2\text{--}7.0 \text{ cm}^{-1}$  and  $2\Delta_{\text{Er}}^z \approx 1.9 \text{ cm}^{-1}$ . This leads to a decrease in the threshold field by more than 50% as compared to the case of pure  $\text{TbFe}_3(\text{BO}_3)_4$  in accordance with the results of experiment (see Fig. 3). At low temperatures, taking into account the inequalities  $\mu_{\text{Er}}^z H_{\text{sf}}$  and  $\Delta_{\text{Er}}^z \ll \Delta_{\text{Er}}^{\perp}$ , we can obtain an expression for the spin-flop transition field analogous to (4),

$$H_{\text{sf}} \approx \frac{N(1-x)\Delta_{\text{Tb}}^z - Nx\Delta_{\text{Er}}^{\perp} - K_{\text{Fe}}/2}{(1-x)N\mu_{\text{Tb}}^z}, \quad (7)$$

which also visually demonstrates a noticeable decrease in  $H_{\text{sf}}$  due to the Er subsystem.

Thus, the simple model proposed here taking into account anisotropy of exchange splitting and  $g$  factors of the fundamental doublets of  $\text{Tb}^{3+}$  and  $\text{Er}^{3+}$  ions makes it possible to describe the observed phase tran-

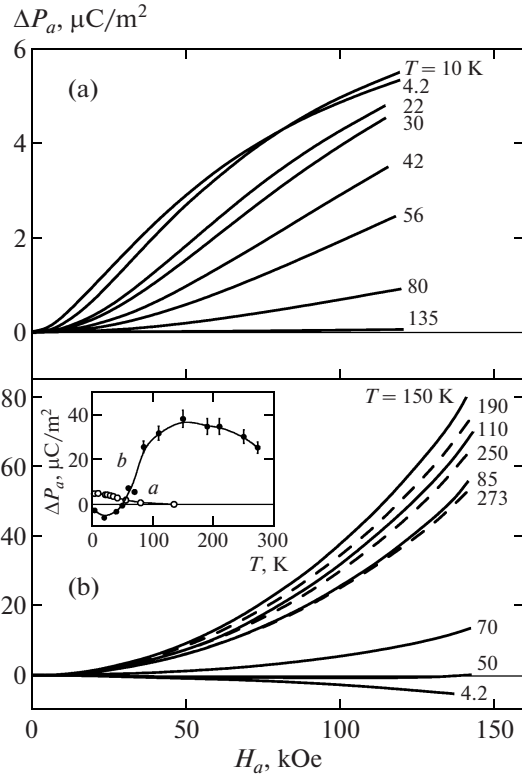


**Fig. 4.** Field dependences of the longitudinal electric polarization along the  $a$  axis in (a)  $\text{Tb}_{0.25}\text{Er}_{0.75}\text{Fe}_3(\text{BO}_3)_4$  and (b)  $\text{TbFe}_3(\text{BO}_3)_4$  at various temperatures. The inset shows the temperature dependences of polarization of these compounds in a fixed magnetic field  $H = 100$  kOe.

sitions in the  $\text{Tb}_{1-x}\text{Er}_x\text{Fe}_3(\text{BO}_3)_4$  system with competing rare-earth contributions.

5. Let us now consider the behavior of electric polarization. It should be noted above all that static measurements of the temperature dependences of pyroelectric current in zero magnetic field revealed an almost complete absence of spontaneous polarization in  $\text{TbFe}_3(\text{BO}_3)_4$  and  $\text{Tb}_{0.25}\text{Er}_{0.75}\text{Fe}_3(\text{BO}_3)_4$  ferroborates. The electric polarization jumps in field  $H_c$  for both compounds were found to be quite small (see Fig. 2b). This is not surprising since, in accordance with the phenomenological theory [1, 2], the electric polarization during the transition to the spin-flop phase is determined by small magnetic field components in the  $ab$  plane, which are not controlled in our experiment and which determine the orientation of the antiferromagnetism vector in this plane (see also [6]).

From this point of view, more informative is the behavior of polarization component  $P_a$  along the  $a$  axis, which is quadratic in a magnetic field, in a magnetic field directed along this axis and inducing no transitions (Fig. 4). It can be seen from Fig. 4b that the behavior of polarization as a function of temperature in  $\text{TbFe}_3(\text{BO}_3)_4$  is quite complex: polarization is small and negative at low temperatures in the magnetically

ordered state. In the region of  $T = 50$  K, the polarization reverses its sign to positive and increases with temperature to values of approximately  $40 \mu\text{C}/\text{m}^2$  in a field of 100 kOe at  $T \approx 150$  K, and then slowly decreases upon a further increase in temperature, remaining quite strong up to room temperatures (see the inset to Fig. 4b). The quadratic magnetoelectric effect at room temperature amounts to about  $\pm 3 \times 10^{-3} \mu\text{C}/\text{m}^2 \text{ kOe}^2$  ( $5 \times 10^{-19} \text{ s/A}$ ), which exceeds the quadratic effects observed in high-temperature multiferroics such as bismuth ferrite ( $>10^{-19} \text{ s/A}$ ) [18] and might be of interest for practical applications (e.g., in developing magnetic electronics and magnetic memory devices). The temperature dependence of polarization indicates a considerable contribution to  $P_a$  from the Tb subsystem, which is controlled at low temperatures by small Van Vleck corrections to the magnetization of  $\text{Tb}^{3+}$  ions perpendicular to the Ising ( $c$ ) axis. With increasing temperature, as the population of excited states of the  $\text{Tb}^{3+}$  ions becomes higher in the crystal field, the contribution of these states reverses the polarization sign and noticeably increases.

Symmetry analysis [2] predicts the existence of contributions to polarization along the  $a$  axis, which are quadratic in the magnetic field:

$$\begin{aligned} \Delta P_a &= c(M_a H_a - M_b H_b) + \dots \\ &= c_1(H_a^2 - H_b^2) + \dots \end{aligned} \quad (8)$$

In contrast to terms of the form  $I_{ij}$ , these contributions also exist at temperatures much higher than the temperature of magnetic ordering of the iron subsystem ( $T_N \approx 40$  K).

This formula shows that the quadratic contribution reverses its sign upon a change in the direction of the field by  $90^\circ$  (from axis  $a$  to axis  $b$ ) without changing its magnitude, which was indeed observed in our experiment (Fig. 5).

In the  $\text{Tb}_{0.25}\text{Er}_{0.75}\text{Fe}_3(\text{BO}_3)_4$  substituted system, the behavior of polarization  $\Delta P_a(H_a, T)$  becomes qualitatively different (see Fig. 4a): it decreases by almost an order of magnitude without reversing its sign and decreases with increasing temperature monotonically. This indicates that the contributions from rare-earth ions to electric polarization apparently associated with the features of their electron structure and spectrum in the crystal field are qualitatively different.

6. Thus, our experiments with  $\text{Tb}_{1-x}\text{Er}_x\text{Fe}_3(\text{BO}_3)_4$  complex ferroborates with competing Tb–Fe and Er–Fe exchange interactions show that magnetic anisotropy, the field of the spin-flop phase transition, and the value of magnetization along the  $c$  axis are controlled by the competition between exchange anisotropic R–Fe contributions and  $g$  factors from the easy-axis (Tb) and easy-plane (Er) subsystems. The simple model proposed here takes into account these features of the ground state of  $\text{Tb}^{3+}$  and  $\text{Er}^{3+}$  ions and

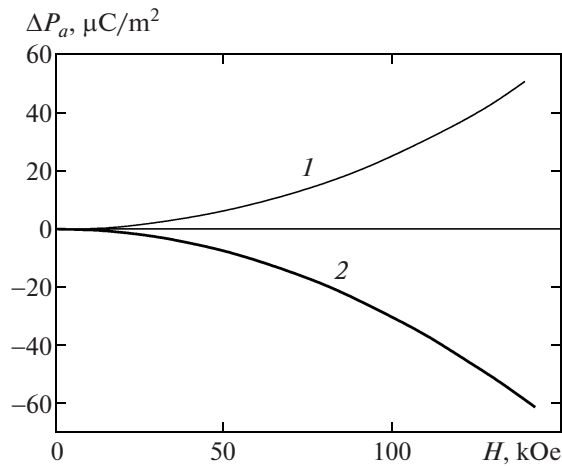


**Fig. 5.** Field dependences of the electric polarization of  $\text{TbFe}_3(\text{BO}_3)_4$  along the  $a$  axis for magnetic field directions along the  $a$  (curve 1) and  $b$  axes (curve 2), illustrating the change in polarization sign upon magnetic field rotation through  $90^\circ$ ;  $T = 273 \text{ K}$ .

makes it possible to describe the observed properties and phase transitions. It has been established that magnetoelectric and magnetostriction anomalies in spin-flop-type transitions are mainly controlled by the Tb subsystem. It is found that the Tb subsystem makes a nonmonotonic contribution to polarization  $P_a(H_a, T)$ , which reverses sign and increases with temperature due to the contribution of excited states of the  $\text{Tb}^{3+}$  ion. The quadratic magnetoelectric effect ( $5 \times 10^{-19} \text{ s/A}$ ) observed in  $\text{TbFe}_3(\text{BO}_3)_4$  at room temperatures changes its sign upon a rotation of the magnetic field through  $90^\circ$  and may be of practical interest for applications.

#### ACKNOWLEDGMENTS

This study was supported by the Russian Foundation for Basic Research (project no. 07-02-00580).

#### REFERENCES

1. A. K. Zvezdin, S. S. Krotov, A. M. Kadomtseva, G. P. Vorob'ev, Yu. F. Popov, A. P. Pyatakov, L. N. Bezmaternykh, and E. A. Popova, *Pis'ma Zh. Éksp. Teor. Fiz.* **81** (6), 335 (2005) [*JETP Lett.* **81** (6), 272 (2005)].
2. A. K. Zvezdin, G. P. Vorob'ev, A. M. Kadomtseva, Yu. F. Popov, A. P. Pyatakov, L. N. Bezmaternykh, A. V. Kuvardin, and E. A. Popova, *Pis'ma Zh. Éksp. Teor. Fiz.* **83** (11), 600 (2006) [*JETP Lett.* **83** (11), 509 (2006)].
3. F. Yen, B. Lorenz, Y. Y. Sun, C. W. Chu, L. N. Bezmaternykh, and A. N. Vasiliev, *Phys. Rev. B: Condens. Matter* **73**, 054435 (2006).

4. A. N. Vasiliev and E. A. Popova, *Fiz. Nizk. Temp. (Kharkov)* **32** (8), 968 (2006) [*Low Temp. Phys.* **32** (8), 735 (2006)].
5. A. M. Kadomtseva, A. K. Zvezdin, A. P. Pyatakov, A. V. Kuvardin, G. P. Vorob'ev, Yu. F. Popov, and L. N. Bezmaternykh, *Zh. Éksp. Teor. Fiz.* **132** (1), 134 (2007) [*JETP* **105** (1), 116 (2007)].
6. A. M. Kadomtseva, Yu. F. Popov, G. P. Vorob'ev, A. A. Mukhin, V. Yu. Ivanov, A. M. Kuz'menko, and L. N. Bezmaternykh, *Pis'ma Zh. Éksp. Teor. Fiz.* **87** (1), 45 (2008) [*JETP Lett.* **87** (1), 39 (2008)].
7. E. A. Popova, N. Tristan, C. Hess, R. Klingeler, B. Büchner, L. N. Bezmaternykh, V. L. Temerov, and A. N. Vasiliev, *Zh. Éksp. Teor. Fiz.* **132** (1), 121 (2007) [*JETP* **105** (1), 105 (2007)].
8. P. Fisher, V. Pomjakushin, D. Sheptyakov, L. Keller, M. Janoschek, B. Roessli, J. Schefer, G. Petrakovskii, L. Bezmaternykh, V. Temerov, and D. Velikanov, *J. Phys.: Condens. Matter* **18**, 7975 (2006).
9. M. N. Popova, E. P. Chukalina, T. N. Stanislavchuk, B. Z. Malkin, A. R. Zakirov, E. Antic-Fidancev, E. A. Popova, L. N. Bezmaternykh, and V. L. Temerov, *Phys. Rev. B: Condens. Matter* **75**, 224435 (2007).
10. D. V. Volkov, A. A. Demidov, and N. P. Kolmakova, *Zh. Éksp. Teor. Fiz.* **131** (6), 1030 (2007) [*JETP* **104** (6), 897 (2007)].
11. E. A. Popova, E. P. Chukalina, T. N. Stanislavchuk, and L. N. Bezmaternykh, *J. Magn. Magn. Mater.* **300**, 440 (2006).
12. E. A. Popova, D. V. Volkov, A. N. Vasiliev, A. A. Demidov, N. P. Kolmakova, I. A. Gudim, L. N. Bezmaternykh, N. Tristan, Yu. Skourski, B. Büchner, C. Hess, and R. Klingeler, *Phys. Rev. B: Condens. Matter* **75**, 224413 (2007).
13. C. Ritter, A. Balaev, A. Vorotynov, G. Petrakovskii, D. Velikanov, V. Temerov and I. Gudim, *J. Phys.: Condens. Matter* **19**, 196 227 (2007).
14. E. A. Popova, N. Tristan, A. N. Vasiliev, V. L. Temerov, L. N. Bezmaternykh, N. Leps, B. Büchner, and R. Klingeler, *Eur. Phys. J., B* **62**, 123 (2008).
15. L. N. Bezmaternykh, S. A. Kharlamova, and V. L. Temerov, *Kristallografiya* **49** (5), 945 (2004) [*Crystallogr. Rep.* **49** (5), 855 (2004)].
16. A. M. Kadomtseva, Yu. F. Popov, G. P. Vorob'ev, K. I. Kamilov, V. Yu. Ivanov, A. A. Mukhin, and A. M. Balbashov, *Zh. Éksp. Teor. Fiz.* **133** (1), 156 (2008) [*JETP* **106** (1), 130 (2008)].
17. V. Yu. Ivanov, A. A. Mukhin, A. M. Kuzmenko, A. A. Pronin, A. M. Kadomtseva, Yu. F. Popov, G. P. Vorob'ev, A. P. Pyatakov, A. K. Zvezdin, and L. N. Bezmaternykh, in *Abstracts of the International Conference "Functional Materials" (ICFM-2007), Partenit, Crimea, Ukraine, October 1–6, 2007* (Partenit, 2007), p. 207.
18. C. Tabares-Munoz, J.-P. Rivera, A. Bezinges, A. Monnier, and H. Schmid, *Jpn. J. Appl. Phys.* **24** (Suppl. 2), 1051 (1985).

*Translated by N. Wadhwa*